

Forecasting the Forced Van der Pol Equation with Frequent Phase Shifts Using a Reservoir Computer

Sho Kuno^{1, a)} and Hiroshi Kori^{1, 2, b)}

¹⁾*Department of Mathematical Informatics, The University of Tokyo, Tokyo, Japan.*

²⁾*Department of Complexity Sciences and Engineering, The University of Tokyo, Kashiwa, Chiba, Japan.*

(Dated: 24 April 2024)

A reservoir computer (RC) is a recurrent neural network (RNN) framework that achieves computational efficiency where only readout layer training is required. Additionally, it effectively predicts nonlinear dynamical system tasks and has various applications. RC is effective for forecasting nonautonomous dynamical systems with gradual changes to the external drive amplitude. This study investigates the predictability of nonautonomous dynamical systems with rapid changes to the phase of the external drive. The forced Van der Pol equation was employed for the base model, implementing forecasting tasks with the RC. The study findings suggest that, despite hidden variables, a nonautonomous dynamical system with rapid changes to the phase of the external drive is predictable. Therefore, RC can offer better schedules for individual shift workers.

I. INTRODUCTION

Nonautonomous dynamical systems are dynamical systems whose evolution is determined by time-variant external drives and parameter effects. These systems are responsive to external effects and time-varying conditions. Thus, they are utilized in various fields, such as physics, biomedical science, ecology, climate, and neuroscience, for modeling phenomena^{1,2}.

The study of the circadian rhythm is a crucial application in the field of biomedical science. The endogenous circadian clock has an oscillation almost synchronized with the light-dark cycle (LD cycle) of the environmental day-night rhythms, with a period of 24 h. The effect of jet lag and constant shift work is inspected by mocking the transition in biological values by a nonautonomous dynamical system with a periodic function as its external drive^{3,4}. However, this classical approach is challenging because building a numerical model that accurately reflects the behavior of the original system is challenging.

Recent trends in the field of machine learning may offer alternative approaches to address the aforementioned issue. The Recurrent neural networks (RNN), a framework of artificial neural networks (ANN), handles the past information and the present input to update its hidden state, enabling it to capture the temporal dependency of the sequential data. For this feature, models of RNN concepts have been effectively utilized in various applications to address problems related to dynamic systems. Long short-term memory (LSTM) addresses the long-term dependency problem and achieves better precision⁵⁻⁹. However, these schemes are inefficient because their training algorithms are time-consuming.

Reservoir Computing (RC), or Echo State Network (ESN), is an innovative framework for RNNs that combines high fidelity in replicating dynamics and efficiency in computation. Owing to its simplified structure, the input, and hidden layers are initialized with a randomly selected matrix, and only the readout layer requires training¹⁰. Further, only a linear regression for the fitting of RC is required, without requiring back-propagation that involves nonlinear computation. This distinguishes RC from the predecessor RNN frameworks. Despite this significant streamlined structure, RC is effective for dynamical systems learning tasks¹¹⁻¹⁴. Furthermore, RC is effective in learning and predicting tasks in nonlinear dynamical systems, which includes results involving nonautonomous dynamical systems. RC can be employed even in chaotic, nonautonomous dynamical systems with a growing amplitude of the external drive¹⁵.

This study aimed to examine the impact of sudden and significant phase shifts on the external drive of the circadian rhythm. We employed a simple oscillator model with a limit cycle to verify the effectiveness of RC in the prediction tasks in the presence of phase shifts. The Van der Pol equation model with a sinusoidal function as the external force was adopted to examine the performance of RC on the forecasting task.

This study is organized as follows: Sec. II describes the formulation of the forced Van der Pol model with the phase shift function. Next, a summary of the RC concept is described. Sec. III compares the results of the forecasts by RC for the number of variables and the training length. Sec. IV discusses the results and the possible application, focusing on the circadian rhythm.

^{a)}Electronic mail: kunosh1225@g.ecc.u-tokyo.ac.jp

^{b)}Electronic mail: kori@k.u-tokyo.ac.jp

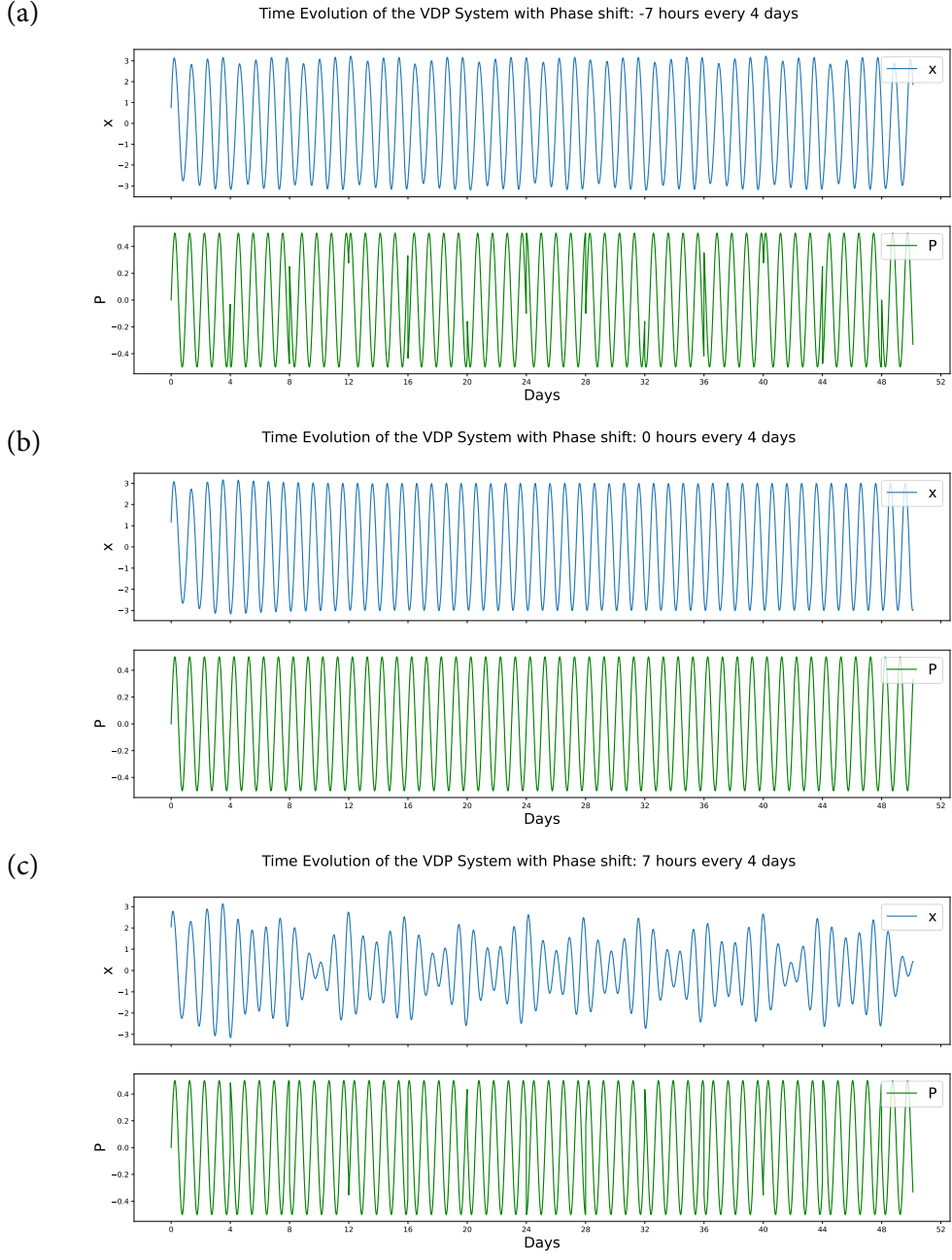


FIG. 1: The variable x and $P_n(t)$ of the time series of the forced Van der Pol equation obtained by a numerical simulation. The phase shift of n hours is injected into the external drive at every 4 d, where (a). $n = -7$. (b). $n = 0$. (c). $n = 7$.

II. METHOD

A. Model

We used the forced Van der Pol model with an external drive $P_n(t)$, expressed as follows:

$$\frac{dx}{dt} = y, \quad (1a)$$

$$\frac{dy}{dt} = \mu(1 - x^2)y - x + P_n(t). \quad (1b)$$

For $P_n(t)$, we chose the following sinusoidal function with a phase shift function $\theta_n(t)$:

$$P_n(t) := A \sin(\Omega t + \theta_n(t)), \quad (2a)$$

$$\theta_n(t) := \frac{n}{24} \left\lfloor \frac{t}{4T_e} \right\rfloor 2\pi. \quad (2b)$$

here, $A = 0.5$ is the amplitude and $\Omega = 1.05$ is the coefficient that scales the period of $P_n(t)$, given by $T_e := \frac{2\pi}{\Omega}$. $\theta_n(t)$ forwards(backwards) the phase of $P_n(t)$ by n hours every 4 d, with $n \in \mathbf{Z}$, $-12 \leq n \leq 12$.

The step size of numerical integration is $h := \frac{T_e}{M}$, where $M = 100$ is the number of divisions. To avoid inconveniences caused by the discontinuity of $P_n(t)$ during the simulation, the data are generated by repeating numerical integrations over the individual intervals between each phase shift and concatenating the obtained time series. Because the $P_n(t)$ phase shift is injected every 4 d, each time series segment has $4M$ time steps, ensuring that the entire time series length is a multiple of this duration. We denote the datasets obtained by simulation as \mathbf{x}^n , where n is the hour of the phase shift to $P_n(t)$. \mathbf{x}^n consists of the value of x, y , and $P_n(t)$ of the forced Van der Pol equation (1). Fig.?? shows the first 50 d of the datasets (only for the variables x and $P_n(t)$) obtained by a simulation for each $n \in \{-7, 0, 7\}$. \mathbf{x}_0 is the forced Van der Pol model without any phase shift to the external drive, whereby the obtained time series is genuinely periodic. When comparing the amplitude of x , the forced Van der Pol equation shows more weakness in the forward shifts than the backward ones. For data simulation, various libraries and modules are available in Python. Thus, we used `scipy.integrate.solve_ivp`. Other options are available in other languages, including `ode45` and `ode15s` in MATLAB.

B. Reservoir Computer

We adopted the basic structure of RC described in 10. The standard model of RC consists of three layers: the input, hidden (reservoir), and readout layers. Let t be the variable for time and denote the data used as the input for updating the reservoir dynamics by \mathbf{z}_t . Define $d_z \in \mathbb{N}$ as the dimension of \mathbf{z}_t . In the input layer, \mathbf{z}_t is mapped to a hidden variable $\mathbf{r}_t \in \mathbb{R}^{d_r}$ of a much higher dimension $d_r > d_z$ inside the hidden layer by a linear transformation \mathbf{W}_{in} of size $d_r \times d_z$,

$$\mathbf{u}_t = \mathbf{W}_{in} \cdot \mathbf{z}_t. \quad (3)$$

In the hidden layer, \mathbf{r}_t is updated by a $d_r \times d_r$ linear transformation \mathbf{W}_r using an activation function $\tanh(\cdot)$. The updating equation of the reservoir state is defined using a variable α of the leaking rate:

$$\mathbf{r}_{t+h} = (1 - \alpha)\mathbf{r}_t + \alpha \tanh(\mathbf{u}_{t+h} + \mathbf{W}_r \cdot \mathbf{r}_t), \quad (4)$$

The leaking rate α is a parameter that controls the effectiveness of the past information on reservoir dynamics, which enables it to regulate the length of the memory RC can store inside. The readout is obtained with another linear transformation \mathbf{W}_{out} of size $d_z \times d_r$,

$$\mathbf{y}_t = \mathbf{W}_{out} \cdot \mathbf{r}_t. \quad (5)$$

As a main feature of RC, the matrices \mathbf{W}_{in} and \mathbf{W}_r are both randomly selected matrices of weights before

the training. \mathbf{W}_{out} is the only part trained to fit the prediction \mathbf{y}_t to \mathbf{z}_t . \mathbf{W}_{out} is obtained by solving a least squares problem of the following form:

$$\mathbf{W}_{out} := \arg \min_{V \in \mathbb{R}^{d_z \times d_r}} \|\mathbf{Z} - \mathbf{V}\mathbf{R}\|_F. \quad (6)$$

To solve this problem, we employ Tikhonov regularization with a regularity parameter $\lambda \geq 0$, which yields a formal solution of the form,

$$\mathbf{W}_{out} := \mathbf{Z}\mathbf{R}^\top (\mathbf{R}\mathbf{R}^\top + \lambda \mathbf{I})^{-1}. \quad (7)$$

C. Procedure

Before the experiment, the datasets \mathbf{x}^n were divided into three consecutive parts: the training, testing, and forecasting periods. The training and testing periods are accessible past information used for training the RC and tuning the hyperparameters. The forecasting period verifies the unknown information about the dynamical system in the future.

The experiment was conducted using the following procedure: First, we optimized the hyperparameters to initialize and train the RC. During this section, we only use the past information without requiring access to the future value of \mathbf{x}^n . During the training and tuning of the hyperparameters, $\mathbf{z}_t := \mathbf{x}_t^n$, representing the value of \mathbf{x}^n at the corresponding time.

$m \in \{n \in \mathbf{Z} \mid -12 \leq n \leq 12\}$ were employed to train the RC with \mathbf{x}_t^m , and the hyperparameters for each m were optimized. We conducted the optimization process by searching for the parameters that achieved the best value for the prediction error during the testing period. We selected the hyperparameters for the fixed m . However, only the training and testing period of the corresponding data \mathbf{x}_t^m was used for the optimization process. Moreover, no future information on the data was accessed during the optimization and training phases.

The forecasting task was conducted with the RC that was initialized using the optimized hyperparameters for m and trained with \mathbf{x}_t^m over the training period. The task forecasts the values of \mathbf{x}_t^n throughout the forecast period, with n being all cases of $-12 \leq n \leq 12$ ($n \neq m$ implies that RC forecasts the state of a dynamical system that it has never experienced). Before forecasting, we warmed up the RC with a last insignificant segment in the testing period of \mathbf{x}^n , contained in the accessible part of the data. Next, in the forecasting phase, RC used its output as the input for the forecast of the next generation, making a loop of input-output. Additionally, we replaced only the input of $P_n(t)$ by the true value, the external drive at that time (see 15 for further discussions). Thus, the input within the forecasting phase could be defined by

$$\mathbf{u}_t := \mathbf{W}_{in} \cdot \mathbf{y}'_t, \quad (8)$$

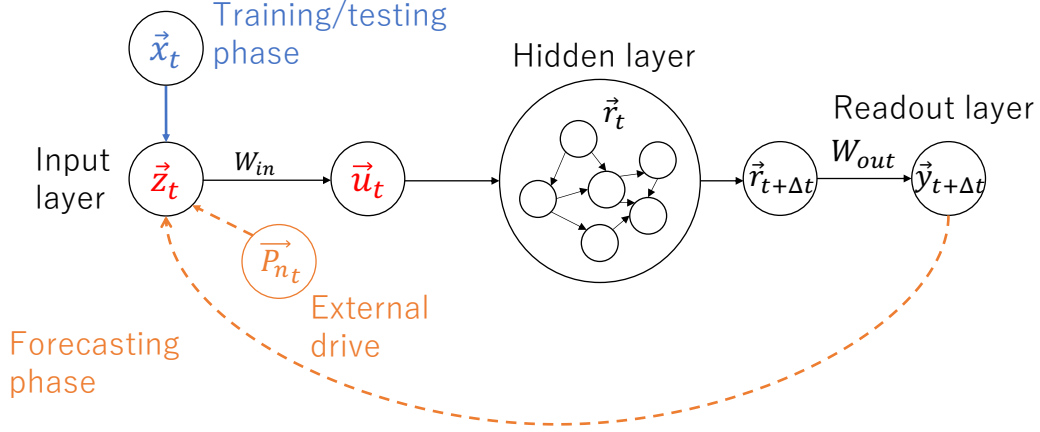


FIG. 2: The basic structure of RC. The input \mathbf{z}_t is mapped onto \mathbf{u}_t in the hidden layer via the matrix \mathbf{W}_{in} . (blue line) During the training and testing period within the optimization of hyperparameters, RC is fed with the true data \mathbf{x}_t of the dynamical system at every step. (orange dashed line) During the forecasting phase, RC updates autonomously using its output as the input for the new step. Here, we inject the true value of the external drive $P_n(t)$ into the input, assuming that $P_n(t)$ is accessible at any time, including the future.

where \mathbf{y}'_t is the vector obtained by substituting the third row of \mathbf{y}_t by the true value of $P_n(t)$. See Fig.2 for the input-output relationship during the forecasting phase.

For the input \mathbf{z}_t , we used array-shaped data with either the values of $x, y, P_n(t)$ or the values of $x, P_n(t)$, assuming that one variable was unobserved. For m , we used $\{-7, 0, 7\}$. The training, testing, and forecast lengths were fixed to 8000, 4000, and 3000 timesteps, respectively. The total datasets were obtained by concatenating these periods. The warmup period was set as the last 10000 timesteps of the testing period.

For the implementation of RC, we used **reservoirpy** in Python¹⁶, with another option available in Python libraries being **PyRCN**¹⁷.

D. Tuning the Hyperparameters

For the training data, we implemented $m \in \{-7, 0, 7\}$. During the optimization process, RC was trained with \mathbf{x}^m over the training period, predicting the state of the dynamical system by one step in the testing period. During the testing period, the estimation error was measured with **NRMSE**:

$$\text{NRMSE}(\mathbf{z}, \mathbf{y}, N) = \sqrt{\frac{\sum_{i=0}^{N-1} (\mathbf{z}_i - \mathbf{y}_i)^2}{N}}. \quad (9)$$

Here, N is the length of the testing period, \mathbf{z} is the input, and \mathbf{y} is the prediction by RC during the testing period.

The hyperparameters were tuned throughout the optimization process to minimize the objective function (9). The set of hyperparameters was **sr** - the spectral radius of the Reservoir layer, **iss** - the input scaling of \mathbf{W}_{in} , **ridge** - the ridge value λ of ridge regression. The search spaces of the hyperparameters were

$[10^{-2}, 10]$, $[0, 1]$, $[10^{-9}, 10^{-2}]$, respectively. Two other major candidates for optimization were the cell number and the leaking rate. However, the cell number was fixed to 500 and the leaking rate to 0.01 for time efficiency during the optimization process.

For the optimization process, we used **Optuna**¹⁸, one of the standard libraries for parameters tuning. Several algorithms for the optimization and pruning processes are provided in the **Optuna**. We used the **optuna.samplers.CmaEsSampler** and **optuna.pruners.SuccessiveHalvingPruner**. Despite the functions varying from **Optuna**, **reservoirpy** is built to be compatible with **hyperopt**¹⁹.

III. RESULTS

A. Hyperparameters

The hyperparameter sets for each case of m are listed in the Appendix. Prediction during the testing period for the case $n = 7$ is shown in Fig. 3.

B. Forecasting

For the dataset, we prepared two types: \mathbf{x}^n and $\hat{\mathbf{x}}^n$. The subarray comprised $x, P_n(t)$ of \mathbf{x}^n . For the first type, the RC was fed with $x, y, P_n(t)$ during the training and testing phases. However, for the second, only $x, P_n(t)$ were available during the same phase. We show the statistical value of the result and calculate the standard deviation of the amplitude of the generated and true data for each n . We plotted the result for each training data in Fig.4 for the results.

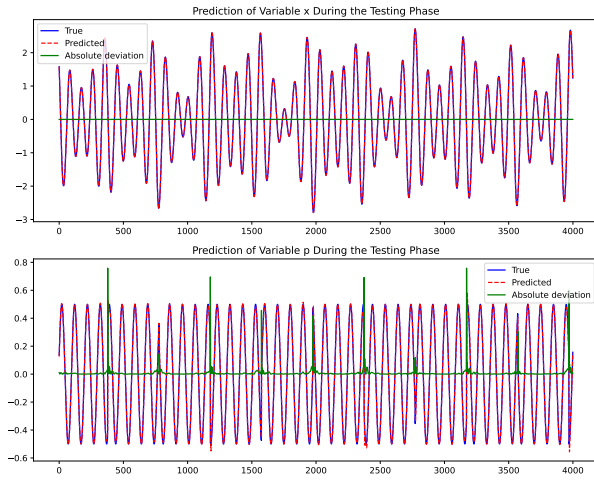


FIG. 3: Prediction by RC of the data x^7 during the testing period. Only the variable x and the external drive $P_n(t)$ are shown.

IV. CONCLUSION AND DISCUSSION

This study demonstrated a forecasting task by RC on the time series of the forced Van der Pol equation with a frequent phase shift to its external drive. To initialize the RC, we chose several shift hours and used the corresponding data to tune the RC hyperparameters. This process requires training the RC with the selected data and minimizing the prediction error during the testing period. The training and testing periods, which include the warm-up period of the time series, provide known information about the dynamics. However, the RC has no access to the data beyond these periods.

The result in Fig. 4 demonstrates the capability of RC to forecast the future state of the forced Van der Pol equation with various phase shifts. Moreover, when RC was fed during the training with the data x^7 , it exhibited a richer pattern, achieving an accurate forecast. When RC used x^0 or x^{-7} , which lacks pattern richness, it yielded reduced fidelity in its forecast. Despite the limited number of observed variables, RC could forecast the future. 15 confirmed chaotic dynamic systems with an external drive whose amplitude increases. Similar results were obtained for a nonautonomous system with a phase shift to its external drive, indicating its applicability to the study of the circadian rhythm.

The variables of the forced Van der Pol equation can be interpreted as the change in the internal state of an organism following the circadian rhythm by regarding the external drive as the LD cycle. Phase shifts in the external drive correspond to the hour of shift work experienced by a shift worker or jetlag. The forecasting performance of RC suggests that the impact of shift work on shiftworker's health can be forecasted with fewer short biological datasets.

Further studies can be designed based on these find-

ings. The circadian rhythm provides the predictability of RC based on real laboratory data. Despite demonstrating the performance of RC with the most basic structure, various advanced versions and RC algorithms exist, such as online learning and the ensemble method^{20,21}. The next-generation reservoir computer is another scheme of RC that achieves enhanced computational efficiency under certain conditions²². Therefore, forecasting tasks via these newer schemes of RC provides future research directions. Theoretical aspects of RC are widely studied^{13,23–26}. Thus, further analysis of the prediction of nonautonomous dynamical systems via RC complements our experimental results. Research on the roles of hyperparameters is of interest, potentially guiding the selection of hyperparameters in various settings, including ours.

- ¹S. Strogatz, *Nonlinear Dynamics and Chaos: With Applications to Physics, Biology, Chemistry, and Engineering* (CRC Press, 2018).
- ²J. Guckenheimer and P. Holmes, *Nonlinear Oscillations, Dynamical Systems, and Bifurcations of Vector Fields*, Applied Mathematical Sciences (Springer New York, 2013).
- ³H. Kori, Y. Yamaguchi, and H. Okamura, "Accelerating recovery from jet lag: Prediction from a multi-oscillator model and its experimental confirmation in model animals," *Sci Rep* **7**, 46702 (2017).
- ⁴Y. Yamaguchi, T. Suzuki, Y. Mizoro, H. Kori, K. Okada, Y. Chen, J.-M. Fustin, F. Yamazaki, N. Mizuguchi, J. Zhang, X. Dong, G. Tsujimoto, Y. Okuno, M. Doi, and H. Okamura, "Mice genetically deficient in vasopressin V1a and V1b receptors are resistant to jet lag," *Science* **342**, 85–90 (2013).
- ⁵N. Mohajerin and S. L. Waslander, "Multistep Prediction of Dynamic Systems With Recurrent Neural Networks," *IEEE Transactions on Neural Networks and Learning Systems* **30**, 3370–3383 (2019).
- ⁶S. Siarni-Namini, N. Tavakoli, and A. S. Namin, "The Performance of LSTM and BiLSTM in Forecasting Time Series," in *2019 IEEE International Conference on Big Data (Big Data)* (2019) pp. 3285–3292.
- ⁷Y. Tan, C. Hu, K. Zhang, K. Zheng, E. A. Davis, and J. S. Park, "LSTM-Based Anomaly Detection for Non-Linear Dynamical System," *IEEE Access* **8**, 103301–103308 (2020).
- ⁸Y. Wang, "A new concept using LSTM Neural Networks for dynamic system identification," in *2017 American Control Conference (ACC)* (2017) pp. 5324–5329.
- ⁹Y. Huang, L. Yang, and Z. Fu, "Reconstructing coupled time series in climate systems using three kinds of machine-learning methods," *Earth System Dynamics* **11**, 835–853 (2020).
- ¹⁰E. Bollt, "On explaining the surprising success of reservoir computing forecaster of chaos? The universal machine learning dynamical system with contrast to VAR and DMD," *Chaos: An Interdisciplinary Journal of Nonlinear Science* **31**, 013108 (2021).
- ¹¹Z. Lu, B. R. Hunt, and E. Ott, "Attractor reconstruction by machine learning," *Chaos: An Interdisciplinary Journal of Nonlinear Science* **28**, 061104 (2018).
- ¹²J. Pathak, B. Hunt, M. Girvan, Z. Lu, and E. Ott, "Model-Free Prediction of Large Spatiotemporally Chaotic Systems from Data: A Reservoir Computing Approach," *Phys. Rev. Lett.* **120**, 024102 (2018).
- ¹³J. Pathak, Z. Lu, B. R. Hunt, M. Girvan, and E. Ott, "Using machine learning to replicate chaotic attractors and calculate Lyapunov exponents from data," *Chaos: An Interdisciplinary Journal of Nonlinear Science* **27**, 121102 (2017).
- ¹⁴P. R. Vlachas, J. Pathak, B. R. Hunt, T. P. Sapsis, M. Girvan, E. Ott, and P. Koumoutsakos, "Backpropagation algorithms and Reservoir Computing in Recurrent Neural Networks for the fore-

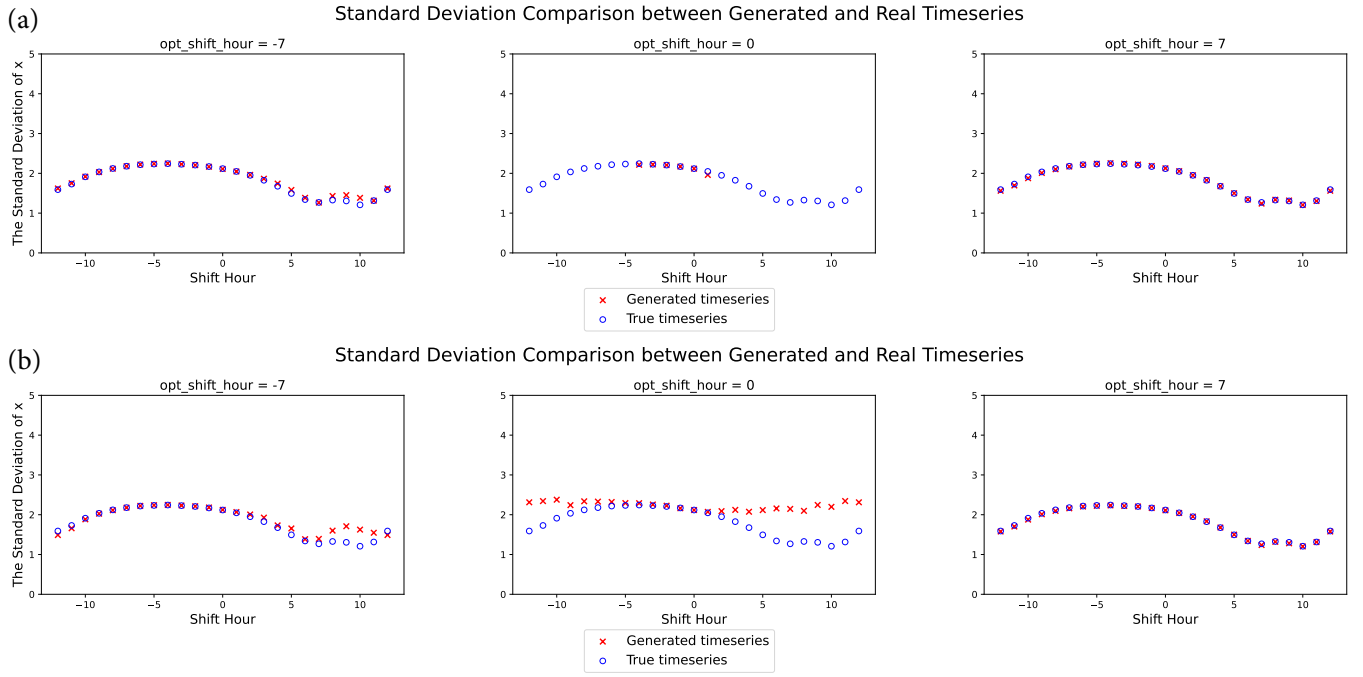


FIG. 4: Standard deviation of the amplitude of the true data and the generated time series, for each of the shift hours added to the phase of the external drive. RC is trained with shift hours $m \in \{-7, 0, 7\}$ to generate time series for dynamics with n hours of phase shift, which is the `opt_shift_hour` in the graph. Both x, y and $P_n(t)$ are used for the input of RC in (a), while in (b), only x and $P_n(t)$ are used.

- casting of complex spatiotemporal dynamics,” *Neural Networks* **126**, 191–217 (2020).
- ¹⁵L.-W. Kong, Y. Weng, B. Glaz, M. Haile, and Y.-C. Lai, “Digital twins of nonlinear dynamical systems,” (2022), [arxiv:2210.06144 \[nlin\]](#).
- ¹⁶N. Trouvain, L. Pedrelli, T. T. Dinh, and X. Hinaut, “ReservoirPy: An Efficient and User-Friendly Library to Design Echo State Networks,” in *Artificial Neural Networks and Machine Learning – ICANN 2020*, Vol. 12397, edited by I. Farkas, P. Masulli, and S. Wermter (Springer International Publishing, Cham, 2020) pp. 494–505.
- ¹⁷P. Steiner, A. Jalalvand, S. Stone, and P. Birkholz, “PyRCN: A Toolbox for Exploration and Application of Reservoir Computing Networks,” (2022), [arxiv:2103.04807 \[cs\]](#).
- ¹⁸T. Akiba, S. Sano, T. Yanase, T. Ohta, and M. Koyama, “Optuna: A Next-generation Hyperparameter Optimization Framework,” (2019), [arxiv:1907.10902 \[cs, stat\]](#).
- ¹⁹J. Bergstra, B. Komer, C. Eliasmith, D. Yamins, and D. D. Cox, “Hyperopt: A Python library for model selection and hyperparameter optimization,” *Comput. Sci. Discov.* **8**, 014008 (2015).
- ²⁰H. Tamura and G. Tanaka, “Partial-FORCE: A fast and robust online training method for recurrent neural networks,” in *2021 International Joint Conference on Neural Networks (IJCNN)* (2021) pp. 1–8.
- ²¹D. Sussillo and L. F. Abbott, “Generating Coherent Patterns of Activity from Chaotic Neural Networks,” *Neuron* **63**, 544–557 (2009).
- ²²D. J. Gauthier, E. Boltt, A. Griffith, and W. A. S. Barbosa, “Next generation reservoir computing,” *Nat Commun* **12**, 5564 (2021).
- ²³L. Grigoryeva, A. Hart, and J.-P. Ortega, “Learning strange attractors with reservoir systems,” *Nonlinearity* **36**, 4674–4708 (2023), [arxiv:2108.05024 \[cs, eess, math\]](#).
- ²⁴X.-Y. Duan, X. Ying, S.-Y. Leng, J. Kurths, W. Lin, and H.-F. Ma, “Embedding theory of reservoir computing and reducing reservoir network using time delays,” *Phys. Rev. Res.* **5**, L022041 (2023).
- ²⁵A. Hart, J. Hook, and J. Dawes, “Embedding and approximation theorems for echo state networks,” *Neural Networks* **128**, 234–247 (2020).
- ²⁶T. Berry and S. Das, “Learning Theory for Dynamical Systems,” *SIAM J. Appl. Dyn. Syst.* **22**, 2082–2122 (2023).